Cirrus Properties Deduced from CO_2 Lidar Observations of Zenith-enhanced Backscatter from Oriented Crystals

Wynn L. Eberhard
NOAA Wave Propagation Laboratory
US Department of Commerce
325 Broadway
Boulder, Colorado 80303

I. Introduction

Many lidar researchers have occasionally observed zenith-enhanced backscatter (ZEB) from middle and high clouds. The ZEB signature consists of strong backscatter when the lidar is pointed directly at zenith and a dramatic decline in backscatter as the zenith angle dips slightly off zenith. Mirror-like reflection from horizontal facets of oriented crystals (especially plates) is generally accepted as the cause. Thomas et al. (1990) found during a 3-year observation program that approximately 50% of ice clouds had ZEB, regardless of cloud height.

The orientation of crystals and the ZEB they cause are important to study and understand for several reasons. First, radiative transfer in clouds with oriented crystals is different than if the same particles were randomly oriented. Second, crystal growth depends partly on the orientation of the particles. Third, ZEB measurements may provide useful information about cirrus microphysical and radiative properties (e.g., Platt et al. 1978 and Eberhard, 1993). And fourth, the remarkable effect of ZEB on lidar signals should be understood in order to properly interpret lidar data.

Laboratory measurements with circular plates (Willmarth et al. 1964) and light pillar data on actual crystals (Sassen 1980), show that ice plates with Reynolds numbers $1 \leq N_{Re} \leq 100$ (or diameters ranging from ≈ 150 to ≈ 2000 μm) orient with the face in the horizontal plane. However, slight angular perturbations of orientation up to a maximum of 0.5-3° have been observed (Platt et al. 1978, Sassen 1980, and Thomas et al. 1990), with minimum perturbations at $N_{Re} \sim 10$ (Sassen 1980).

Circular cylinders in the laboratory (Jayaweera and Mason 1965) oriented with the long axis horizontal when $0.1 \leq N_{Re} \leq N_{Re,max}$, where $N_{Re,max}$ increases as the length-to-diameter ratio increases. Figure 1 shows the range of ice columns that are expected to orient expressed in terms of longest dimension (i.e., axis length) L. It is not known whether hexagonal cylinders show any tendency to orient in the roll direction such that one

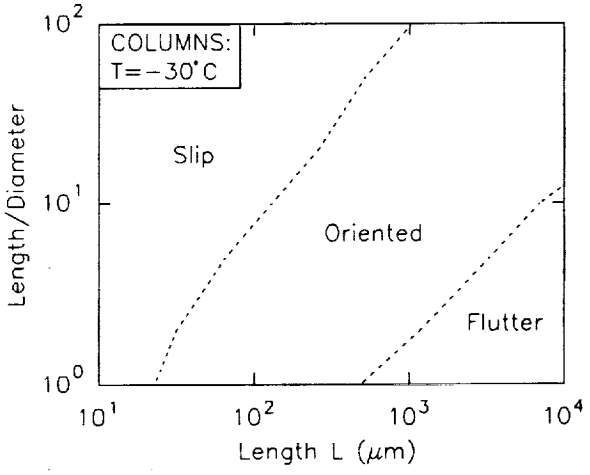

Fig. 1. Domain of sizes of hexagonal columns expected to orient with the long axis horizontal based on Reynolds-number-scaled laboratory measurements of circular cylinders.

of the six faces around the hexagon remains in the horizontal plane.

The 10.6-μm-wavelength CO_2 lidar that operated during FIRE II frequently scanned about the zenith to study the ZEB phenomenon. A companion paper (Eberhard, 1993) describes the scattering models developed for interpreting the measurements, and this paper describes some interpretations of the data using those models.

II. ZEB for CO_2 lidar

The lidar scanned in elevation angle in a plane aligned with the wind direction at cloud height. Averages were made for several scans, typically over a 500-s period, to smooth out most of the variations in cloud density. Clouds were divided into vertical layers within which the elevation-angle-dependent shape of the average ZEB signal was consistent. Average backscatter as a function of lidar elevation angle was calculated for each layer. Figure 2 shows some typical signatures from 26 November 1991 that illustrate different kinds of ZEB signatures, which depend on several factors that are explained in this section.

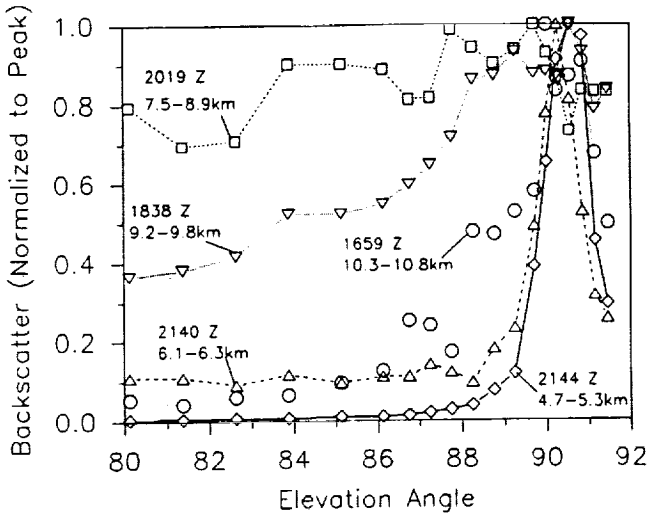

Fig. 2. Typical ZEB observations as a function of CO_2 lidar elevation angle. Times are GMT on 26 November 1991, and heights are ASL.

Clouds composed only of plates have very strong backscatter at zenith with very little backscatter in the wings far from the peak (see curve A in Fig. 1 of Eberhard 1993). Therefore, the curve for 2144 Z in Fig. 2 suggests the presence of oriented plates. According to the model in Eberhard (1993), the zenith enhancement from plates is so strong that even the small signal in the wing of the curve indicates that only 12% of the cloud (as weighted by the cross sectional area of the particles) is composed of oriented plates. In comparison, we infer that 3.5% of the particles at 1659 Z are oriented plates.

Clouds containing only perfectly shaped and horizontally oriented columns, but with random roll orientation, have less zenith enhancement and much more backscatter in the wings (curve C in Fig. 1 of Eberhard 1993) than plates have. The curve at 2140 Z in Fig. 2 might be a mixture of 30% oriented columns and 70% randomly oriented particles, but it also could be a mixture of 0.2% oriented plates and 98.8 randomly oriented particles. The data from 2144 and 1659 Z have larger peak-to-shoulder ratios than permitted by the cylinder model, but an ambiguity exists for oriented crystal type in the data at 2140 Z.

The data at 2019 Z are an example of data that decline so little with zenith angle that we infer negligible ZEB and 100% randomly oriented particles for the layer.

The width of the peak for perfectly oriented plates with truly flat faces depends on diffraction, with peak width proportional to wavelength and inversely proportional to plate diameter. The same is true, except for a numerical factor, for perfectly oriented columns with random roll orientation. In either case, the width of the peak reveals the size of the longest dimension of oriented particles. However, the peak can be additionally widened by nondiffraction factors, such as slight fluttering motions, optical imperfections, and shape imperfections that alter the stable orientation slightly from one particle to the next. Therefore, an estimate of the size of oriented particles using the width of the peak gives only a lower bound on the long dimension. Diffraction and nondiffraction factors can both be significant at 10.6-μm wavelength, whereas the nondiffraction factors dominate the width of the ZEB peak for lidars with a wavelength $\leq$ 1.5 μm. If plates are assumed for the curves at 2144 and 2140 Z in Fig. 2, the lower bound on diameters are 197 and 246 μm, respectively. If the oriented particles at 1659 and 1838 Z were plates, there must have been significant nondiffractive spreading, because the inferred lower bounds on plate diameters are only 93 and 42 μm, respectively, which are smaller than the limit for orientation discussed in the introduction. If the oriented particles for these two cases were columns, it is not clear whether nondiffractive spreading was a factor.

III. Statistics from 26 November 1991

Statistics on ZEB parameters for the period 1657-2151 Z on 26 November 1991 are compiled in Figs.

3-5. The scanning data from this period were divided vertically and temporally as described in Section II into 72 cases.

The distribution of the peak-to-shoulder ratio is shown in Fig. 3, where the peak value is the maximum

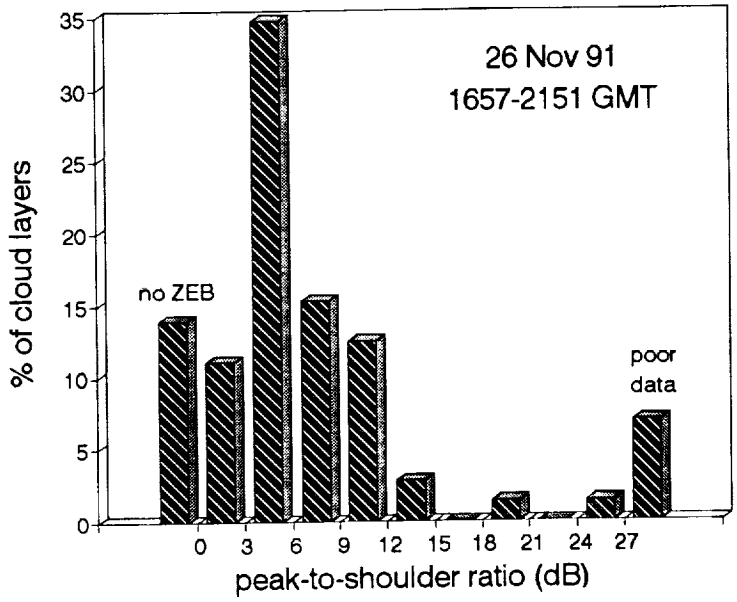

Fig. 3. Probability distribution of the strength of the ZEB signature for height- and time-averaged cloud segments.

backscatter near zenith, and the shoulder value is that at the lowest elevation angle (usually 80°). Poor data (optically thick intervening cloud or extreme patchiness) prevented analysis in five of the cases. ZEB was observed in 57 (or 85%) of the remaining cases. However, the peak-to-shoulder ratio was less than 6 dB in more than half the cases.

Assuming plates in the 57 cases with ZEB, Fig. 4 shows the distribution of the inferred lower bound on

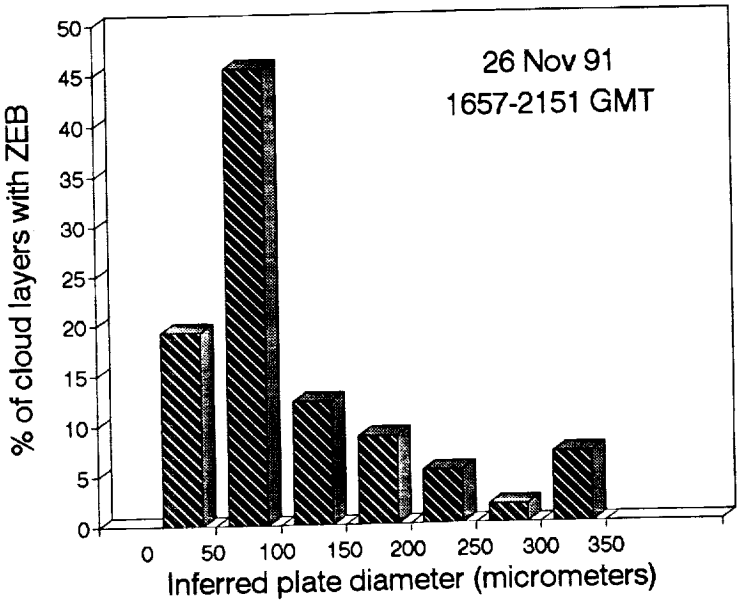

Fig. 4. Inferred lower bound of the largest dimension of oriented particles (assuming plates) for the 57 cases with ZEB.

plate diameter. More than half of the inferred diameters are less than 100 μm, i.e., less than the lower Reynolds-number limit for plate orientation. We infer nondiffractive spreading of the ZEB peak from plates or the presence of short columns rather than plates for these cases.

Figure 5 gives the statistics on the fraction of cloud, weighted by particles' cross-sectional area, composed of oriented particles. The results depend dramatically on whether plates or columns are in the cloud. Thirteen (or 18%) of the cases have ZEB strong enough that plates must be dominating the ZEB. However, the

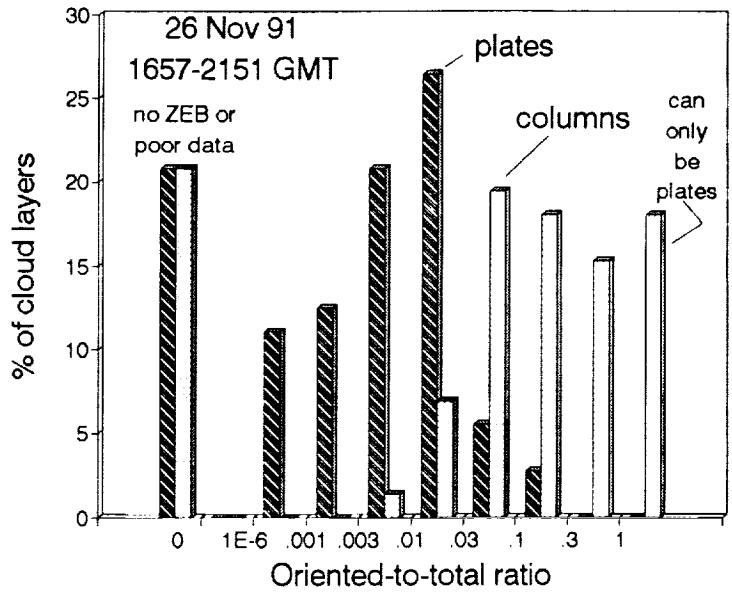

Fig. 5. Fraction of cloud composed of oriented particles (weighted according to cross sectional area) according to whether plates or columns are assumed.

model (Eberhard 1993) indicates that no more than 13% of the particles are oriented plates in any of the cases. Forty-four (or 61%) of the cases could consist partly of columns comprising cloud fraction ranging from nearly 100% to less than 1%.

IV. Discussion

The CO_2 lidar data from a 5-h period on 26 November 1991 frequently had ZEB, even more often than the more comprehensive data set of Thomas et al. (1990). The enhancement was small for most cases during the 5-h period, so adjusted lidar backscatter cross sections (Eberhard 1993) can be used with confidence for this portion of the data. The inferred diameters of the oriented particles (assuming plates) are often smaller than the range predicted from laboratory simulations, which is consistent with the expectation that nondiffractive spreading will often bias results to smaller diameters. The nondiffractive spreading of the peak and the ambiguities between different mixtures of plates, columns, and randomly oriented particles pose major problems in intrepreting ZEB data.

Future research will examine ZEB for the entire FIRE II data set and investigate whether temperature data can be used to infer the growth habit of oriented crystals to remove the plate-column ambiguity. Lidar ZEB results will be compared with simultaneous replicator and 2-D image measurements in an attempt to confirm and refine the interpretation of the ZEB signatures.

Acknowledgments. My thanks go to coworkers in Wave Propagation Laboratory for assistance in data acquisition and to B. Gordon, M. Jung and J. Bevilacqua for data processing and graphics.

V. References

Eberhard, W.L., 1993: Progress in interpreting CO_2 lidar signatures to obtain cirrus microphysical and optical properties. (this volume).

Jayaweera, K.O.L.F., and B.J. Mason, 1965: The behaviour of freely falling cylinders and cones in a viscous fluid. *J. Fluid Mech.*, **22**, 709-720.

Platt, C.M.R., N.L. Abshire, and G.T. McNice, 1978: Some microphysical properties of an ice cloud from lidar observation of horizontally oriented crystals. *J. Appl. Meteor.*, **17**, 1220-1224.

Sassen, K., 1980: Remote sensing of planar ice crystal fall attitudes. *J. Meteor. Soc. Japan*, **58**, 422-429.

Thomas, L., J.C. Cartwright, and D.P. Wareing, 1990: Lidar observations of the horizontal orientation of ice crystals in cirrus clouds. *Tellus*, **42B**, 211-216.

Willmarth, W.W., N.E. Hawk, and R.L. Harvey, 1964: Steady and unsteady motions and wakes of freely falling disks. *Phys. Fluids*, **7**, 197-208.